

First-principles Modeling of Plasmons in Aluminum under Ambient and Extreme Conditions

Kushal Ramakrishna, Attila Cangi, Tobias Dornheim, Andrew Baczewski, Jan Vorberger

41st workshop on High-Energy-Density Physics with laser and ion beams
February 1st 2021

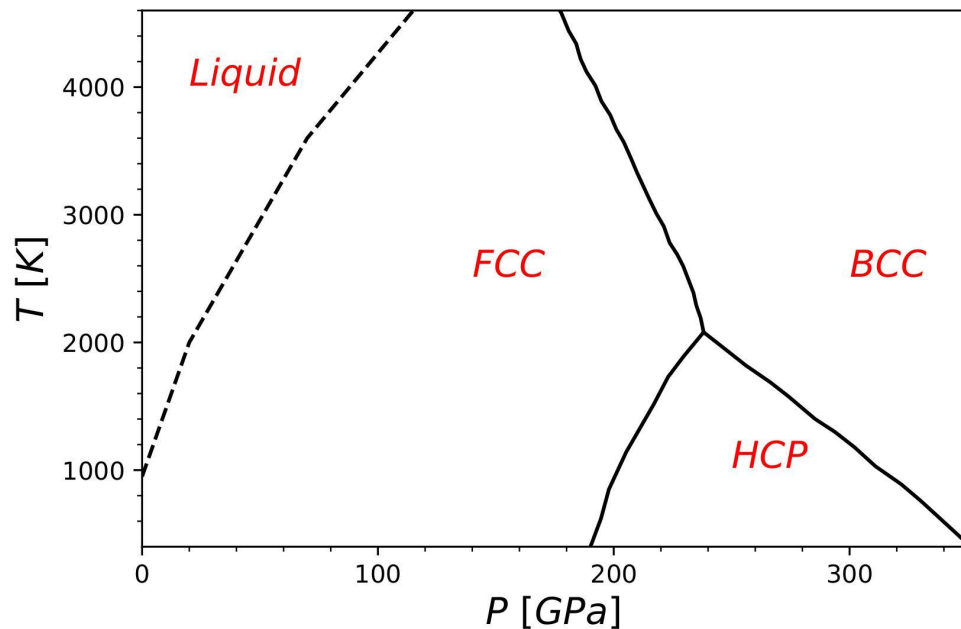


www.casus.science



Outline

- An assessment of several state-of-the-art modeling techniques to predict plasmon properties, both under ambient and warm dense conditions.
- The numerical modeling techniques tested include dielectric models based on static local field corrections (LFC) obtained using path integral Monte Carlo (PIMC) data for the uniform electron gas (UEG) at ground state and finite temperature.
- Linear response time-dependent density functional theory (TDDFT) as well as adiabatic exchange-correlation approximations (ALDA).
- Computation of properties such as dynamic structure factor, static structure factor, plasmon dispersion and plasmon width and compared to measurements on aluminum accessible via electron energy-loss spectroscopy (EELS), inelastic X-ray scattering (IXS) and X-ray Thomson scattering (XRTS).



- At standard temperature and pressure, solid aluminum adopts a fcc crystal structure with a density of 2.7 g/cm^3 and $r_s=2.07$.
- Density of states resembling the free electron gas, one would expect the plasmon dispersion to be described well by the random phase approximation (RPA).

- The linear response of the electronic system to an external, time-dependent perturbation δv is given in Fourier space by

$$n_{ind}(\mathbf{q}, \omega) = \chi(\mathbf{q}, \omega) \delta v(\mathbf{q}, \omega)$$

- density-density response function $\chi(\mathbf{q}, \omega)$
$$\frac{1}{\epsilon(\mathbf{q}, \omega)} = 1 + \frac{4\pi}{q^2} \chi(\mathbf{q}, \omega)$$

- Fluctuation-dissipation theorem connects the DSF to the density-density response function

$$S(\mathbf{q}, \omega) = -\frac{1}{\pi n_e (1 - e^{-\omega/(k_B T_e)})} \text{Im} [\chi(\mathbf{q}, \omega)] = -\frac{q^2}{4\pi^2 n_e (1 - e^{-\omega/(k_B T)})} \text{Im} [\epsilon^{-1}(\mathbf{q}, \omega)]$$

- Using the detailed balance relation for the DSF, diagnostics of parameters in experiments such as the temperature, the equation of state, and the density are inferred.

$$S(-\mathbf{q}, -\omega) = S(\mathbf{q}, \omega) e^{-\beta \hbar \omega}$$

- Random-Phase Approximation (RPA)

Simplest approximation capable of describing collective properties of a system of weakly interacting electrons (jellium model) immersed in a uniform positively charged background.

$$\Im[\epsilon(q, \omega)] = (2s_e^z + 1) \frac{4\pi m^2 e^2 k_B T}{\hbar q^3} \times \ln \left\{ \frac{1 + \exp \left\{ \beta \left(-\frac{E^-}{2m} + \mu \right) \right\}}{1 + \exp \left\{ \beta \left(-\frac{E^+}{2m} + \mu \right) \right\}} \right\}$$

$$E^\pm = (\pm q/2 - m\hbar\omega/q)^2$$

$$\omega^2(q) = \omega_{pl}^2 \left[1 + \frac{\langle p^2 \rangle}{m^2} \frac{q^2}{\omega^2(0)} + \frac{\langle p^4 \rangle}{m^4} \frac{q^4}{\omega^4(0)} + \dots \right]$$

Thiele et al. PRE 78, 026411 (2008)

Reinholz et al. PRE 62, 56485666 (2000); Fortmann et al. Phys. Rev. E 81, 026405 (2010)

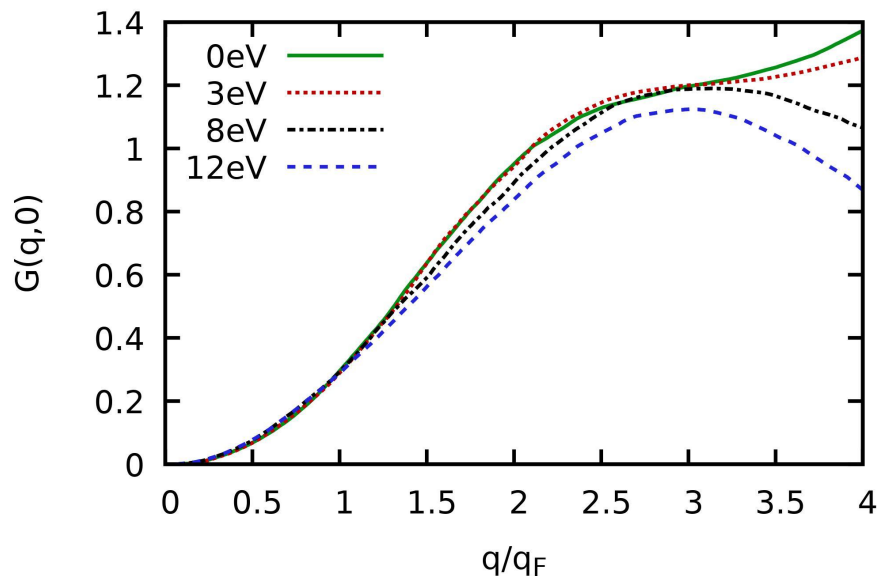
- Extended Mermin dielectric function

The RPA is not sufficient to account for strong correlations and the jellium model is not sufficient to account for bound states.

Introducing a dynamic damping or relaxation term leads to the Mermin approach (MA), which takes into account electron-ion collisions.

$$\epsilon^{MA}(q, \omega) = 1 + \frac{[1 + i\nu(\omega)/\omega] [\epsilon(q, \omega + i\nu(\omega)) - 1]}{1 + \left[i \frac{\nu(\omega)}{\omega} \right] \frac{\epsilon(q, \omega + i\nu(\omega)) - 1}{\epsilon(q, \omega \rightarrow 0) - 1}}$$

Theoretical methods: Local field corrections



- Based on *ab initio* path-integral Monte-Carlo (PIMC) data for the warm dense electron gas to include , electron-electron correlations.
- Improved results for electronic properties like $S(q, \omega)$, $S(q)$, without any additional computational cost.

$$\chi(q, \omega) = \frac{\chi^0(q, \omega)}{1 - V(q) [1 - G(q, \omega)] \chi^0(q, \omega)}$$

- In the static limit, replace $G(q, r_s, \Theta)$

Corradini et al. PRB 57, 14569-14571 (1998)

Dornheim et al. JCP 151, 194104 (2019)

Dornheim et al. PRL 125, 235001 (2020)



Talk by Tobias Dornheim, February 2nd 11:00

- Solving a set of Kohn-Sham equations for the KS orbitals

$$\left[-\frac{1}{2} \nabla_{\mathbf{k}}^2 + V_S(\mathbf{r}) \right] \phi_{\mathbf{k}}(\mathbf{r}) = \epsilon_{\mathbf{k}} \phi_{\mathbf{k}}(\mathbf{r})$$

- Evaluate Kohn-Sham density-density response function

$$\chi_{\mathcal{G}\mathcal{G}'}^{KS}(\mathbf{q}, \omega) = \frac{\chi_{\mathcal{G}\mathcal{G}'}^{KS}(\mathbf{q}, \omega)}{1 - [V(\mathbf{q}) + f_{XC}(\mathbf{q}, \omega)] \chi_{\mathcal{G}\mathcal{G}'}^{KS}(\mathbf{q}, \omega)}$$

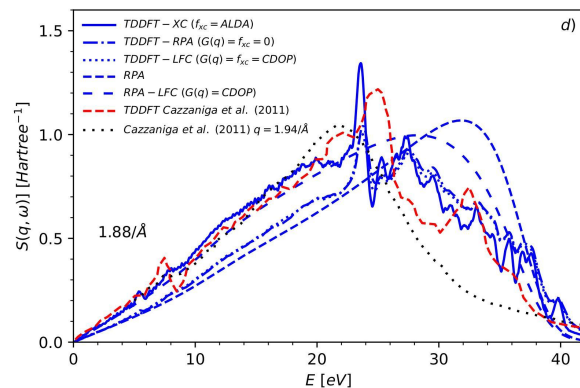
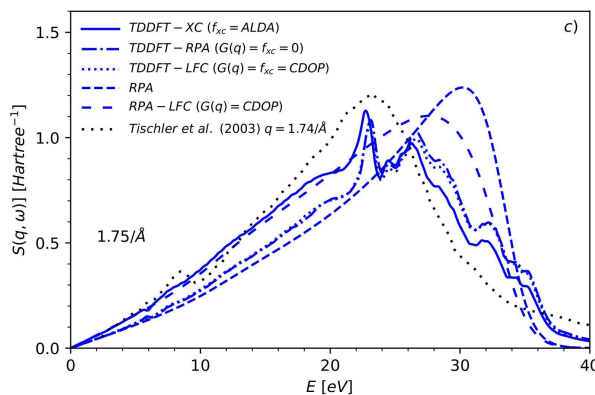
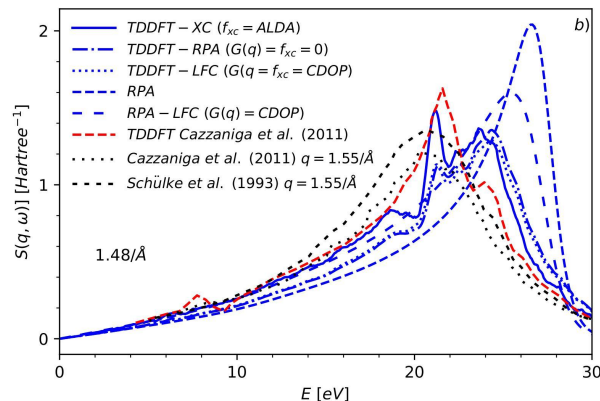
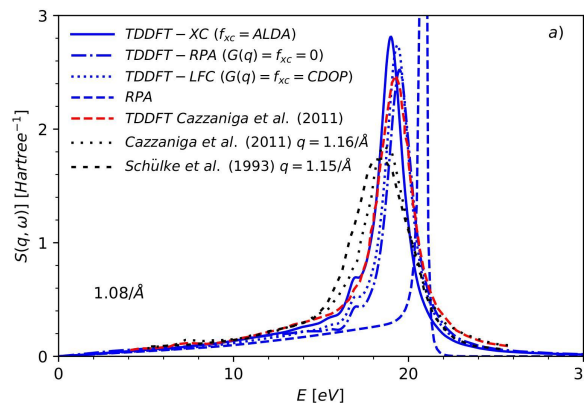
$$\chi_{\mathcal{G}\mathcal{G}'}^{KS}(\mathbf{q}, \omega) = -\frac{1}{V} \lim_{\eta \rightarrow 0^+} \sum_{nm; \mathbf{k}} [f_{m; \mathbf{k}+\mathbf{q}}(T) - f_{n; \mathbf{k}}(T)]$$

$$\times \frac{\langle \psi_{m; \mathbf{k}+\mathbf{q}} | e^{i(\mathbf{q}+\mathcal{G})\mathbf{r}} | \psi_{n; \mathbf{k}} \rangle \langle \psi_{n; \mathbf{k}} | e^{-i(\mathbf{q}+\mathcal{G}')\mathbf{r}'} | \psi_{m; \mathbf{k}+\mathbf{q}} \rangle}{\omega - \epsilon_{m; \mathbf{k}+\mathbf{q}} + \epsilon_{n; \mathbf{k}} + i\eta}$$

- $f_{XC}(\mathbf{q}, \omega)$ is the exchange-correlation kernel $f_{XC}(\mathbf{q}, \omega) = \chi^{KS-1}(\mathbf{q}, \omega) - \chi^{-1}(\mathbf{q}, \omega) - v(\mathbf{q})$ $f_{XC}(\mathbf{q}, \omega) = \frac{\delta v_{xc}(\mathbf{q}, \omega)}{\delta n(\mathbf{q}, \omega)}$

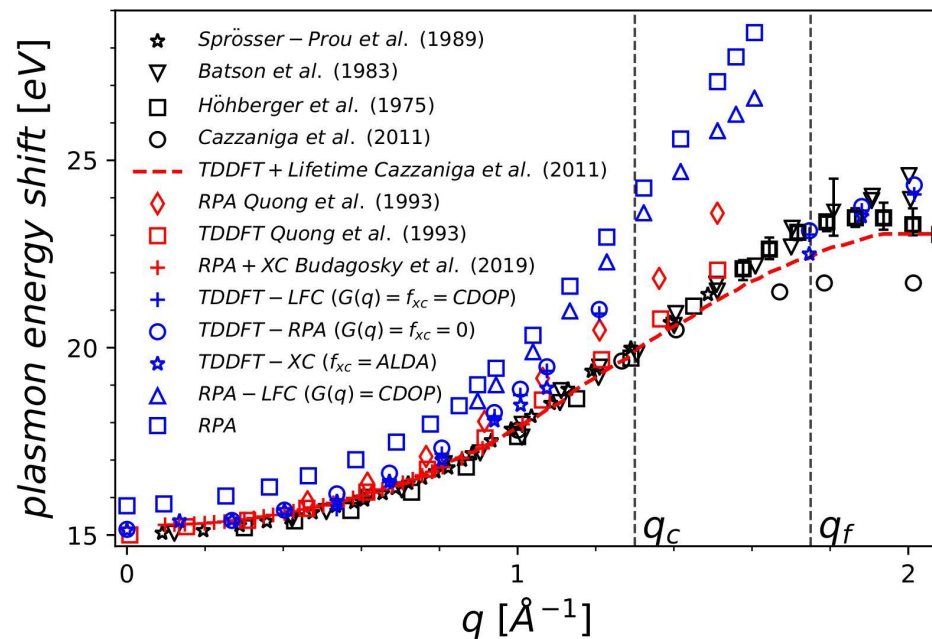
- Usually evaluated using the adiabatic local density approximation (TDDFT-XC, ALDA). $f_{XC} \rightarrow 0$ yields what is called RPA calculations within the TDDFT framework (TDDFT-RPA). With LFC obtained from QMC calculations leads to (TDDFT-LFC).

Ambient conditions: Dynamic structure factor



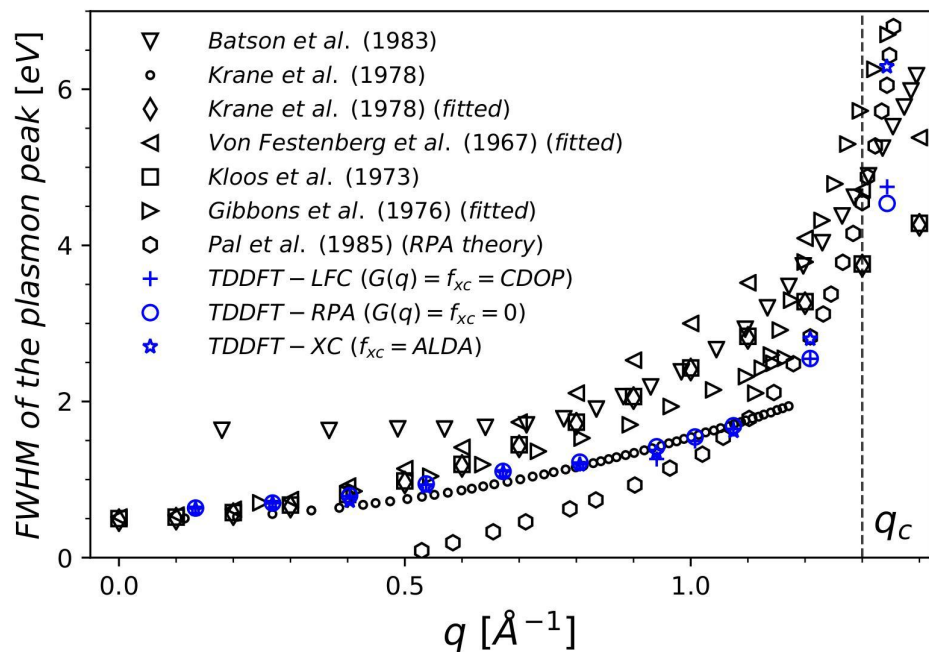
- At small q , the system is clearly dominated by collective effects, and the sharp plasmon carries most of the spectral weight.
- TDDFT results suggests deviations from a free electron model due to the lattice.
- Increasing the wavenumber of the perturbation leads to a broadening of the plasmon peak and finally to a mix of collective and single-particle effects.
- A two peak structure, as it seems to emerge from TDDFT at the higher wavenumbers, is associated with plasmon and double plasmon excitations absent in the experimental curves.

Ambient conditions: Plasmon dispersion

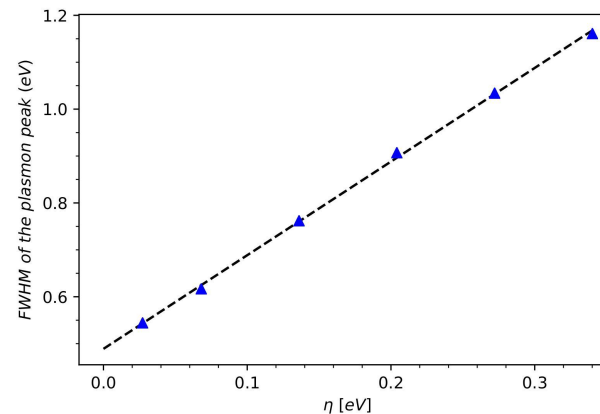


- Shift is based on the location of the peak of the DSF.
- For small q , the various TDDFT approaches agree well with the theoretical results and the experimental measurements.
- Near q_c , we start to see deviations between experiment and different theoretical results.
- The inclusion of different LFCs (TDDFT-LFC, CDOP Corradini et al), and XC Kernels (TDDFT-XC) results in a lowering of the plasmon shift at intermediate and large q .

Ambient conditions: Plasmon lifetimes

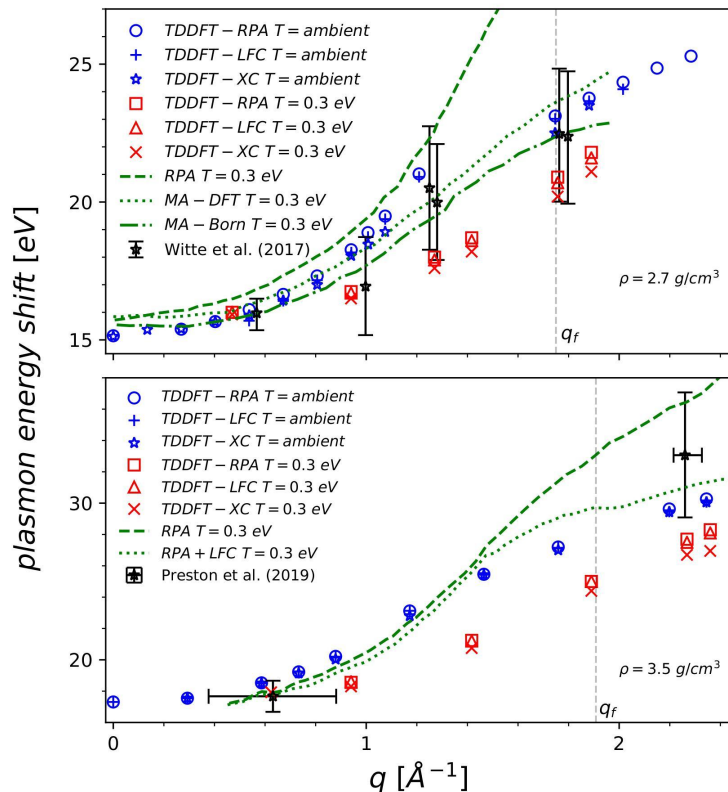


- FWHMs computed using LR-TDDFT depend on the Lorentzian broadening η .



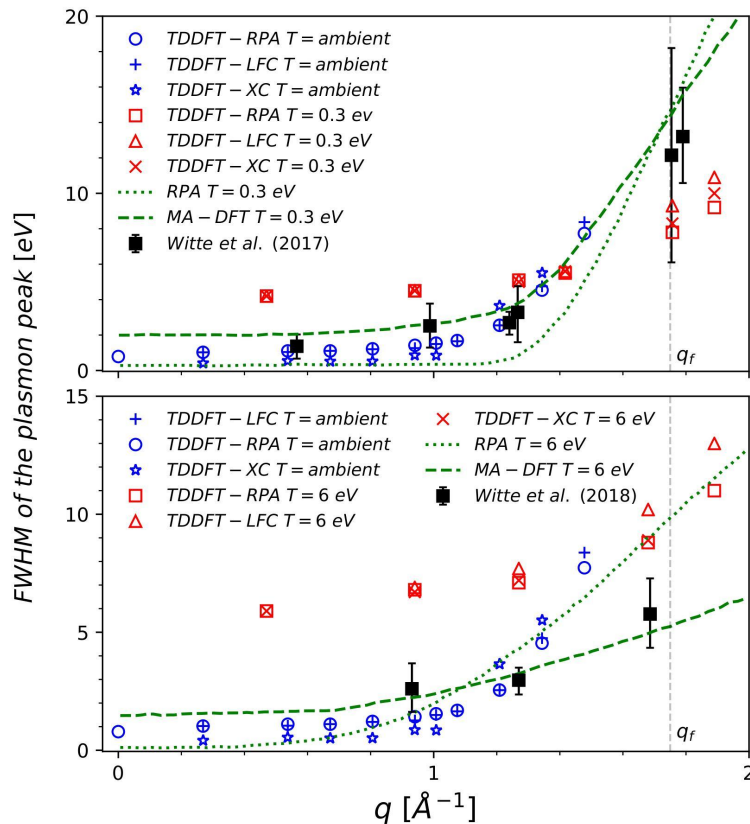
- Plasmon lifetime results are in good agreement with the experimental results at small q .
- Significant deviations near q_c when the LFC has an increasing impact.

Extreme conditions: Plasmon dispersion



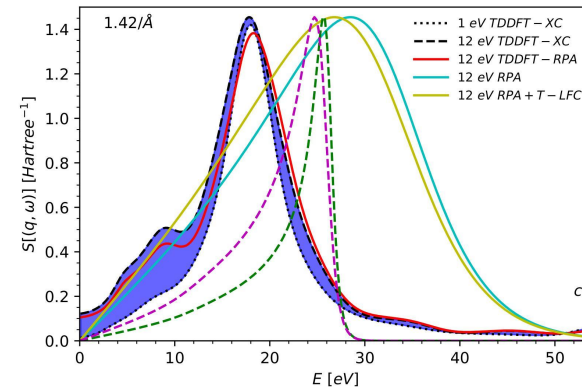
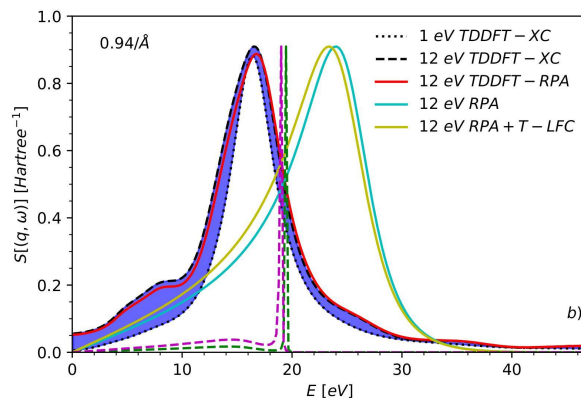
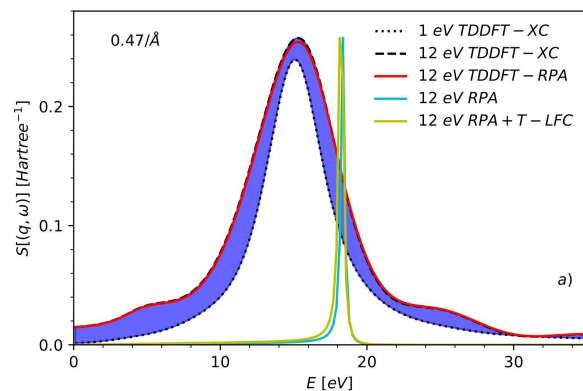
- For small wavenumbers, TDDFT results agree well with the experimental and other curves, which is mainly an indication that the density is correct.
- At larger wavenumbers, deviations are apparent which are caused by differing temperatures and different levels of approximations.
- A better agreement is reached when considering the ions at ideal lattice positions and not in a molten state.
- The ambient data is in much better agreement with both XRTS measurements than the results obtained at $T = 0.3 \text{ eV}$

Extreme conditions: Plasmon lifetimes



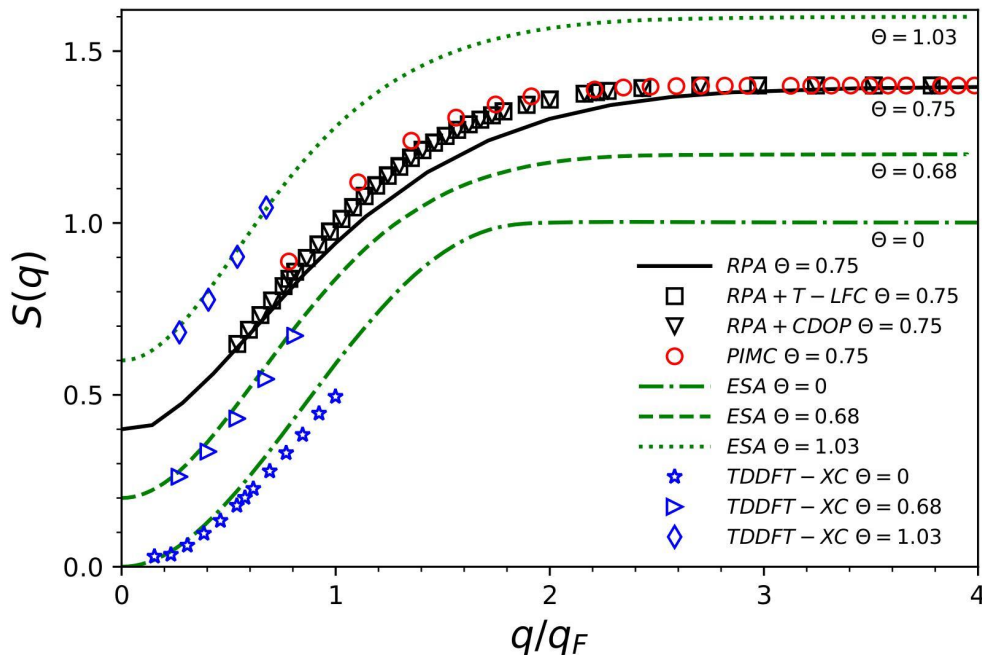
- At higher temperatures, the TDDFT results feature larger widths for small q but the data still lies within the large error bars of the experimental results at large q .
- Ambient data is in much better agreement with the XRTS measurements than results at 0.3 eV and 6 eV.

Extreme conditions: Temperature Dependence of the DSF



- Temperature results in an increase of width of the plasmon peak.
- For TDDFT, the locations of the peaks at a specific q are independent of temperature. This is contrary to the prediction of the Lindhard-RPA for which the energy of the plasmon changes drastically with temperature.
- The temperature determination from the plasmon peak and width is highly model dependent and great care should be taken in the choice of the applied theory.

Static structure factor



- An important test of the quality of the DSF is given by the calculation of several different moments of the structure factor.

$$S(q) = \int_{-\infty}^{\infty} S(q, \omega) d\omega$$

- The agreement between the integrated TDDFT spectra and the static structure from both PIMC and ESA is very good and can serve as a benchmark of the quality of the TDDFT spectra.

Dornheim et al. JCP 151, 194104 (2019)

Dornheim et al. PRL 125, 235001 (2020)

- Numerical modeling of WDM is challenging due to the electron-electron correlation and ionic structure under relatively high temperature and pressure.
- Starting from TDDFT-RPA, we used a variety of XC kernels in the LR-TDDFT equations: ALDA, static ($T = 0$) LFC, and temperature-dependent LFC.
- We demonstrate the capabilities of LR-TDDFT in calculating plasmon dispersion and plasmon lifetimes for the simple metal aluminum at ambient and extreme conditions.
- Our assessment clearly points to a strong need for the development or improvements in reliable methods such as in LR-TDDFT.
- Important for the evaluation of experimental spectra from XRTS and other experiments, because such spectra are also used for temperature and density determination.
- **Goal: Benchmark novel exchange-correlation kernel which is also temperature-dependent and relevant for WDM.**